


A new Bi(III)-based coordination complex: Treatment and nursing application values on pediatric pneumonia

Progress in Reaction Kinetics and Mechanism
2021, Vol. 46(0) 1–10
© The Author(s) 2021
Article reuse guidelines:
sagepub.com/journals-permissions
DOI: 10.1177/14686783211045834
journals.sagepub.com/home/prk


Jianli Lu¹, Hong Han¹, Bo Li² and Yanjun Han¹

Abstract

In the current work, through applying the mixed-ligand generation method, $[\text{Bi}_4\text{Cl}_8(\text{PDC})_2(2,2'\text{-bpy})_4]\cdot 2\text{MeCN}$ (**1**), a fresh bismuth (III)-organic compound synthesized with the solvothermal reactions between 2,2'-bipyridine (2,2'-bpy); 2,6-pyridinedicarboxylic acid (H_2PDC); and bismuth chloride. The structural characterization results show that complex **1** features a binuclear discrete structure which is further extended into a 1D chain-like supramolecular network via π - π interactions. Furthermore, the compound's treatment and nursing application values on pediatric pneumonia was explored and the novel compound's corresponding mechanism was also investigated. First of all, in our research, the enzyme-linked immunosorbent assay (ELISA) detection kit was employed for the determination of the inflammatory cytokines content released into alveolar lavage fluid. Subsequently, the adenosine 5'-monophosphate (AMP)-activated protein kinase (AMPK) signaling pathway activation in alveolar epithelial cells was explored exploiting the real-time reverse transcription-polymerase chain reaction (RT-PCR). Molecular docking demonstrated that although multiple pyridine rings are presented in the Bi complex, however, only the carboxylate groups have been observed to interact with the active residues.

Keywords

Coordination complex, pediatric pneumonia, (AMP)-activated protein kinase signaling pathway, molecular docking

¹Department of Pediatrics, Xingtai People's Hospital, Xingtai, Hebei, China

²Department of Cardiology, Children's Hospital of Hebei Province, China

Corresponding author:

Yanjun Han, Department of Pediatrics, Xingtai People's Hospital, 16 Hongxing Street, Xiangdu District, Xingtai 054031, Hebei Province, China.

Email: hanyj12305@163.com



Creative Commons Non Commercial CC BY-NC: This article is distributed under the terms of the Creative Commons Attribution-NonCommercial 4.0 License (<https://creativecommons.org/licenses/by-nc/4.0/>) which permits non-commercial use, reproduction and distribution of the work without further

permission provided the original work is attributed as specified on the SAGE and Open Access pages (<https://us.sagepub.com/en-us/nam/open-access-at-sage>).

Introduction

Mycoplasma pneumoniae is a common pathogen of respiratory system infections. It is mainly transmitted through respiratory droplets and can infect throughout the year, and the incidence is relatively high in winter and spring.¹ *Mycoplasma pneumoniae* can cause respiratory diseases in children and can cause extrapulmonary complications. In recent years, the incidence of *Mycoplasma pneumoniae* pneumonia (MPP) in children has been increasing year by year, which has attracted more and more scholars' attention.^{2,3} The pathogenesis of MPP in children has been understood, but the mechanism is still not very clear. Understanding the pathogenesis of MPP could provide a theoretical basis for clinical prevention and treatment.

For the supramolecular structures including the metal in view of crystal engineering, their design and the architecture are causing widespread concern in the coordination and supramolecular chemistry areas. The reason why people pay increasing attention to these areas is because of their significant unit in architecture; at the same time, they have extensive application prospects in luminescence and biochemistry along with the catalysis field, especially in the areas of modern pharmaceutical chemistry.⁴⁻⁶ In the various compounds we have created, the functional complexes have gained extensive interest because of their great pharmaceutical value. As a result, in design of architecture and drug therapy along with the clinical employment, the key factor is to choose an efficient, safe, as well as biocompatible ligand.⁷⁻⁹ The polydentate ligands involving the heterocyclic ligands containing N atoms and the polycarboxylic acids have been widely exploited in these multifunctional complexes' controlled synthesis along with their reasonable design. In the last few years, the nitrogen-heterocyclic carboxylic acid ligands have been extensively studied by biologists and chemists on the account of their various functional performances and coordination fashions, together with their H-bonding acceptors and donors with the conditions of solution.¹⁰⁻¹⁵ Nevertheless, bismuth along with the materials based on bismuth is widely employed in photocatalysts, pharmaceuticals, as well as other materials in solid condition on account of their fascinating characteristics such as low cost and high thermodynamic stability, together with non-toxicity.¹⁶ In the current work, by applying the mixed-ligand generation method, $[\text{Bi}_4\text{Cl}_8(\text{PDC})_2(2,2'\text{-bpy})_4]\cdot 2\text{MeCN}$ (**1**), a fresh bismuth (III)-organic compound is synthesized with the solvothermal reactions between 2,2'-bipyridine (2,2'-bpy); 2,6-pyridinedicarboxylic acid (H_2PDC , Scheme 1); and bismuth chloride. The **1**'s architecture was detected by exploiting the EA together with the diffraction of single-crystal X-ray. Serial biological experiments were conducted in the experiment for the novel compound's bio-activity evaluation and the details of its mechanism were explored at the same time. The ELISA detection results reflected that our compound could obviously down-regulate the inflammatory cytokines released into the alveolar lavage fluid, dose-dependently. In addition to this, this compound also remarkably inhibited the AMPK signaling pathway activation in alveolar epithelial cells in a dose-dependent fashion. In addition, molecular docking simulation is utilized to analyze the latent interactions between the chosen receptor protein and Bi complex.

Experimental

Chemicals and measurements

All of the reagents along with solvents employed in our investigation could be acquired from the market, and they were used without processing. The FT-IR spectra could be performed utilizing KBr pellets (with the sample of 5 mg in 500 mg KBr) with the infrared spectra region ranging from

400 cm^{-1} to 4000 cm^{-1} . By utilizing the analyzer of PerkinElmer 2400 C, the analysis of hydrogen, nitrogen, and carbon elements was implemented.

Preparation and characterization of $[\text{Bi}_4\text{Cl}_8(\text{PDC})_2(2,2'\text{-bpy})_4]\cdot 2\text{MeCN}$ (I)

0.0313 g and 0.1 mmol of bismuth chloride; 2.6–0.1 mmol and 0.0165 g of pyridinedicarboxylic acid; 0.0150 g and 0.1 mmol of 2,2'-bipyridine; and 3 mL of acetonitrile were put into a stainless-steel autoclave lined with polytetrafluoroethylene. The autoclave was heated in an oven at a constant temperature statically for 24 hours at 150°, and then this autoclave was removed from the oven; and finally, it could cool gradually to environmental temperature for more than 4 h. The container of reaction was allowed to stand for a week to harvest the product; the product was then cleaned by using ethanol and then it was dried under environmental conditions. The complex 1's colorless crystals with thick needles' shape were formed. The complex 1's estimated yield is 36% (according to Bi). Elemental analysis for the $\text{C}_{56}\text{H}_{41}\text{Bi}_4\text{Cl}_8\text{N}_{11}\text{O}_8$: Calc. (Obs.): N, 7.28% (7.17%); C, 34.79% (34.95%); and H, 1.95% (1.74%). IR (KBr pallet, cm^{-1} , [Supplementary Figure S1](#)): 3354 (s), 2836 (m), 1600 (s), 1551 (s), 1506 (m), 1490 (m), 1455 (s), 1433 (m), 1386 (m), 1366 (m), 1337 (s), 1312 (s), 1180 (w), 1149 (m), 1108 (s), 1008 (w), 947 (w), 907 (w), 843 (m), 769 (m), 737 (m), 707 (m), 687 (m), 613 (w), 598 (w), 562 (w), and 491 (m).

The data for X-ray can be analyzed through Oxford Xcalibur E diffractometer. For the strength data, it was analyzed via the CrysAlis Pro, and this data was then converted to HKL files. The original structural manners were established by the direct mean-based SHELXS, and after that, least-squares method-based SHELXL-2014 was used for modification. The anisotropic parameters were mixed with global non-hydrogen atoms. Next, the entire hydrogen atoms were geometrically fixed via applying the AFIX commands to carbon atoms that they adjacent to. The compound's details of optimization and its parameters of crystallography were revealed in length in the [Table 1](#).

ELISA assay

ELISA was implemented in our investigation to detect the inflammatory cytokines released into the alveolar lavage fluid after treatment with the compound. This implementation was finished fully according to the instructions' guidance with minor modifications.¹⁷ Shortly, the animals used in this research were provided via the Model Animal Center of Nanjing University (Nanjing, China). Before performing this treatment, all of the mice were kept between 20°C and 25°C temperature, with free water and food. The pediatric pneumonia animal model was constructed by infection with *Pseudomonas aeruginosa*, and the compound was exploited to accomplish treatment at 1, 2, and 5 mg/kg concentration. The fluid of alveolar lavage was harvested and the inflammatory cytokine content (i.e., TNF- α and IL-1 β) was measured. This experiment was implemented more than three times. Finally, the acquired information was reflected as mean \pm SD

Real-time RT-PCR

The in-depth real-time RT-PCR was completed in the investigation in order to explore the AMPK signaling pathway activation in alveolar epithelial cells after the treatment with this compound and the generation of the animal model of pediatric pneumonia. This investigation was also implemented in line with the instructions with some modifications.¹⁸ Shortly, the animal model of pediatric pneumonia was established by infection with *Pseudomonas aeruginosa*, and the treatment was finished after adding this compound with 1, 2, and 5 mg/kg concentration. Afterward, in the

Table I. The complex's details of optimization and their parameters of crystallography.

Empirical formula	$C_{56}H_{41}Bi_4Cl_8N_{11}O_8$
Formula weight	2115.52
Temperature/K	99.99
Crystal system	Triclinic
Space group	P-1
a/Å	9.6239 (3)
b/Å	13.6678 (5)
c/Å	27.3126 (11)
$\alpha/^\circ$	102.5246 (10)
$\beta/^\circ$	90.628 (2)
$\gamma/^\circ$	110.674 (4)
Volume/Å ³	3266.2 (2)
Z	2
$\rho_{\text{calc}}/\text{g}/\text{cm}^3$	2.151
μ/mm^{-1}	11.130
Data/restraints/parameters	16348/0/785
Goodness-of-fit on F^2	1.099
Final R indexes [$I \geq 2\sigma(I)$]	$R_1 = 0.0277$, $\omega R_2 = 0.0626$
Final R indexes [all data]	$R_1 = 0.0426$, $\omega R_2 = 0.0660$
Largest diff. Peak/hole/e Å ⁻³	3.15/−1.25
CCDC	2,078,365

mice, alveolar epithelial cells could be isolated and in alveolar epithelial cells, the overall RNA could be extracted by utilizing the reagent TRIzol. After the measurement of the entire RNA quantity and quality, it was reverse transcribed into cDNA. In alveolar epithelial cells, the AMPK signaling pathway activation was explored, and the *gapdh* was exploited as a control gene.

Simulation methods. For implementing the molecular docking simulation, a family member of AMP-activated protein kinase (AMPK) has been employed; the corresponding PDB ID is 3KH5, and it possesses a fresh AMP-binding position which has been referred to as site E. Site E is situated in the small binding pocket between alpha-helices.¹⁹ The structure is downloaded from the protein data bank, the existing water molecules, and other ligands.

Then AutoDockTools (1.5.6) has been utilized to construct the binding grid parameter file, in which the grid center is defined as the center of mass of 3KH5 receptor protein and the length of the grid is 60 Å. Next, the docking parameter file has also been prepared with the help of AutoDockTools, although the Bi complex has been set as semi-flexible ligand; however, none of the rotating dihedrals has been presented. 50 possible binding poses have been allowed during the scoring procedure. All molecular docking simulations were performed by AutoDock (4.2).

Results and discussion

Structural characterization

The **1**'s architecture in solid condition is constructed via eight chloride ions, four distinctive bismuth (III) ions in crystallography, two ligands of PDC, and four bidentate ligands of 2,2'-bpy. Both the

Bi1 and the Bi3 are 7-coordinated; they are bound with two O atoms that come from the ligand of PDC, 2 N atoms in a κ^2 -2,2'-bpy, and three chloride ions. The spacing of Bi1–O is 2.7644 (2) Å and 2.5498 (2) Å, the lengths of Bi1–Cl are between 2.508 (2) Å and 2.744 (2) Å, and the distances of Bi1–N are 2.465 (2) Å and 2.435 (2) Å. Nevertheless, with the Bi3, the separations of Bi3–O are 2.781 (2) Å and 2.552 (2) Å, the distances of Bi3–Cl are between 2.640 (2) Å and 2.660 (2) Å, and the lengths of Bi3–N are 2.472 (2) Å and 2.431 (2) Å. Both the Bi2 and the Bi4 are 6-coordinated; they are bound with two O atoms that originate from the ligand of PDC, 3 N atoms in a ligand of κ^2 -2,2'-bpy and a PDC, and a chloride ion. The separations of Bi2–O are 2.263 (1) Å and 2.549 (2) Å and the lengths of Bi2–N are between 2.508 (2) Å and 2.549 (2) Å. The spacing of Bi2–Cl14 is 2.474 (2) Å, while the two long interactions of Bi–Cl are found to be 3.4579 (2) Å and 3.2081 (2) Å. The lengths of Bi4–O are 2.2811 (1) Å and 2.5633 (2) Å, and the separations of Bi4–N are between 2.4271 (2) Å and 2.5745 (2) Å. The spacing of Bi4–Cl8 is 2.4917 (2) Å, while the two long interactions of Bi–Cl are found to be 3.4905 (2) Å and 3.2147 (2) Å. The Bi1 and the Bi2 are connected together with a O atom (namely, O52) of the PDC ligand carboxylic acid to produce the dimeric units. The pseudo-tetramers were generated via the interaction of these dimers via two chloride atoms (i.e., Cl13 and Cl12) as illustrated in the Figure 1(a). Similarly, the Bi3 and the Bi4 are connected together through a PDC ligand carboxylic acid (namely, O62) to produce the dimeric

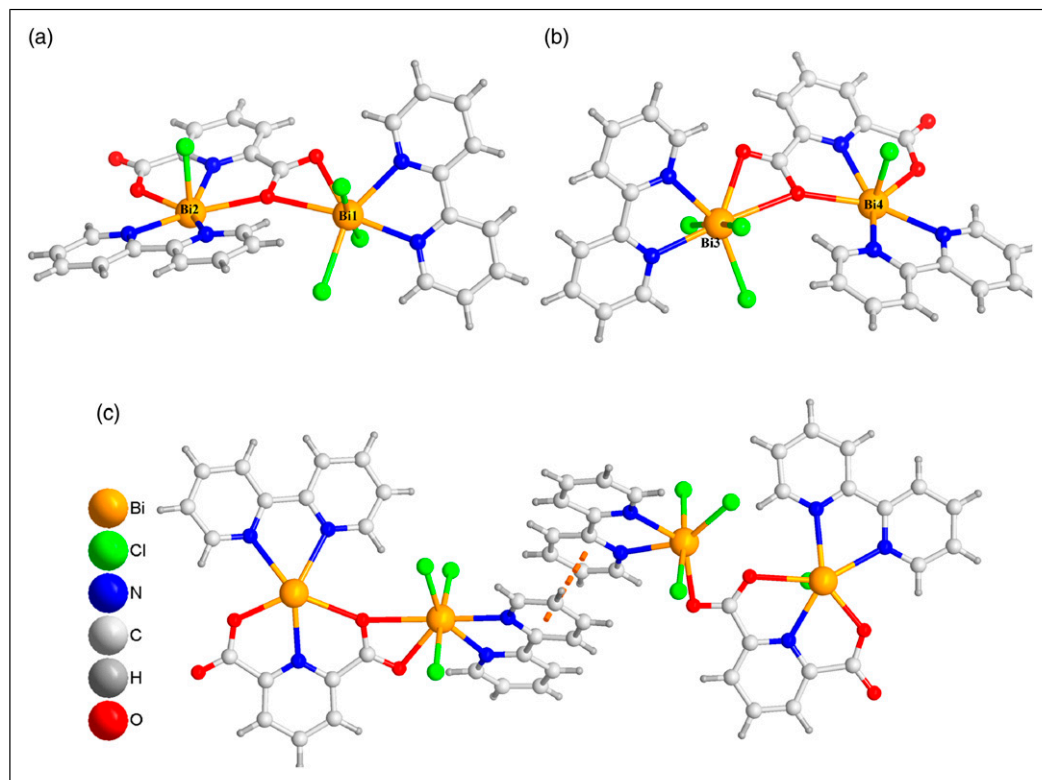


Figure 1. (a) The coordination surrounding view of Bi2 and Bi1 in complex I. (b) The coordination surrounding view of B4 and Bi3 in the complex I. (c) The interactions of π - π stacking between the consecutive discrete structures.

units, which is then linked in-depth into the pseudotetramers via a relatively long interaction of Bi–Cl–Bi containing two chlorine atoms (i.e., Cl7 and Cl6). In the process of refinement, each molecular formula unit possesses an outer coordination sphere, and the acetonitrile molecule is decomposed, and there exists a density of residual electrons outside the cluster. This density of residual electrons is probably owing to an extra molecule of ACN; nevertheless, the disorder hinders these atoms' modeling, and the pattern is compressed to remove the density of residual electrons. Several interactions of π – π in the molecular form are found between the pyridine ring and phen ring of pseudo-tetramers, which stabilizes in-depth the crystal architecture. As displayed in Figure 1(c), there are moderate interactions of π – π stacking between the ligands of 2,2'-bpy bound to Bi3 and Bi1.

Compound could significantly reduce the release of the inflammatory cytokines into the alveolar lavage fluid

After creating the fresh compound with new architecture, the novel compound's treatment and nursing application values against pediatric pneumonia were explored. As a result, the ELISA detection kit was used, and the content of inflammatory cytokines released into the alveolar lavage fluid was determined. As the results reflect in Figure 2, it can be observed that the model group has a higher content level of the inflammatory cytokines released into the alveolar lavage fluid in contrast to the control group. After the treatment with the compound, the inflammatory cytokine levels in the alveolar lavage fluid were reduced in a dose-dependent manner.

Compound obviously inhibited the activation of the AMPK signaling pathway in the alveolar epithelial cells

In the previous exploration, we have demonstrated that this compound could evidently reduce the inflammatory cytokine levels released into alveolar lavage fluid. As the signaling pathway of

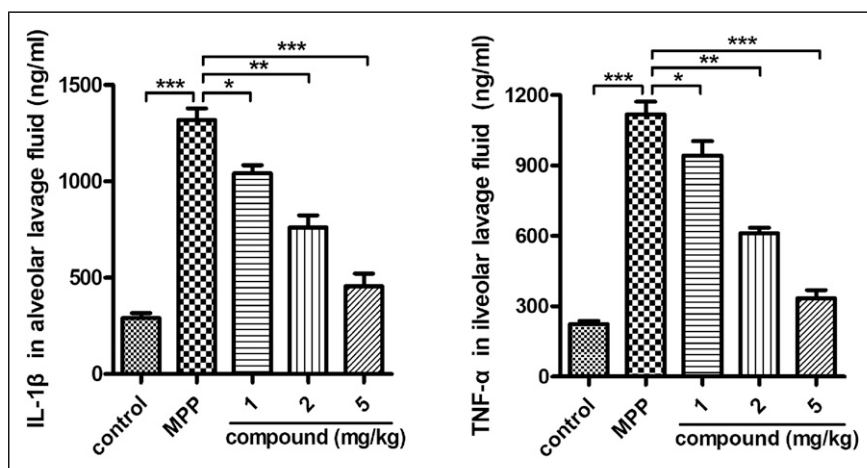


Figure 2. Significantly reduced inflammatory cytokines levels' release into alveolar lavage fluid. The animal model of pediatric pneumonia was created and the treatment was carried out after adding this compound with 1, 2, and 5 mg/kg concentration. The alveolar lavage fluid was harvested and the inflammatory cytokines content was determined. * means $p < 0.05$, ** means $p < 0.01$, and *** means $p < 0.005$.

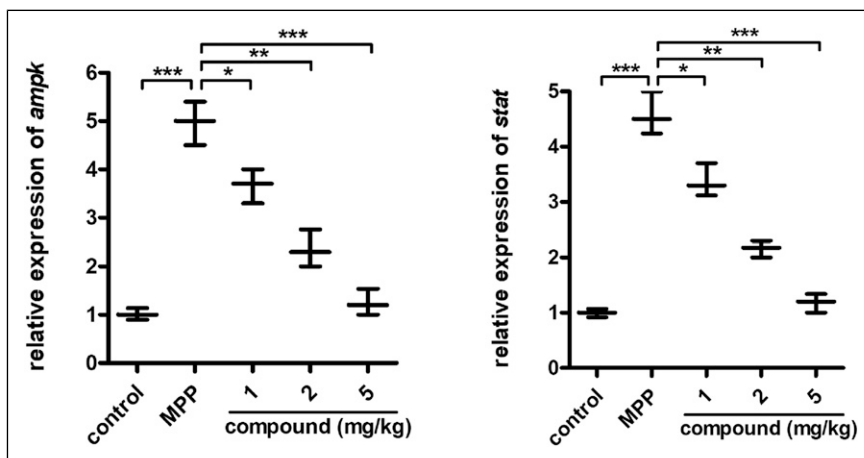


Figure 3. Obviously inhibited AMPK signaling pathway activation in alveolar epithelial cells after treating with this complex. The pediatric pneumonia animal model was constructed and the compound was employed in order to finish the treatment at 1, 2, and 5 mg/kg concentration. The alveolar epithelial cells were harvested, and the AMPK signaling pathway activation in alveolar epithelial cells was measured via applying the real time RT-PCR. * means $p < 0.05$, ** means $p < 0.01$, and *** means $p < 0.005$.

AMPK regulates the inflammatory cytokines release, the real-time RT-PCR was carried out for the detection of the AMPK signaling pathway activation in alveolar epithelial cells. The data in the Figure 3 reflect that the model group exhibits much higher levels of AMPK activation in comparison with control group, with p value less than 0.005. After treating with this compound, the AMPK signaling pathway activation level in alveolar epithelial cells was down-regulated in a dose-dependent manner.

Molecular docking

On account of the protein of AMP-activated protein kinase (AMPK) including two regulatory subunits and a kinase subunit, it has been frequently used as receptor protein for signaling and screening biological capabilities of the proposed pharmaceutical molecules.¹⁷ Thus, as a family member of the AMPK protein family, 3KH5 has been utilized for investigating the biological activity of the synthesized Bi complex. The calculated binding conformation that has the lowest affinity energy has been displayed in Figure 4; the estimated affinity energy is -6.95 kcal/mol, with a measured inhibition constant of 8.0 μM .

From the binding conformation, it can be observed that only one binding interaction is formed between the Bi complex and 3KH5 receptor protein. The interacting active residue is GLY116 and the length of the formed hydrogen bond is 3.33 Å. Further, it can be seen that the oxygen from the carboxyl group is the donator of the hydrogen bond. Besides the carboxyl groups, there are three pyridine groups on the Bi complex; however, none of them could form binding interaction with the active residues like GLY117, MET55, VAL115, etc. It can be explained that all the nitrogen atoms in the pyridine groups have strong interaction with the central Bi ion and therefore cannot further interact with the surrounding active residues. The above results demonstrated that only the carboxyl

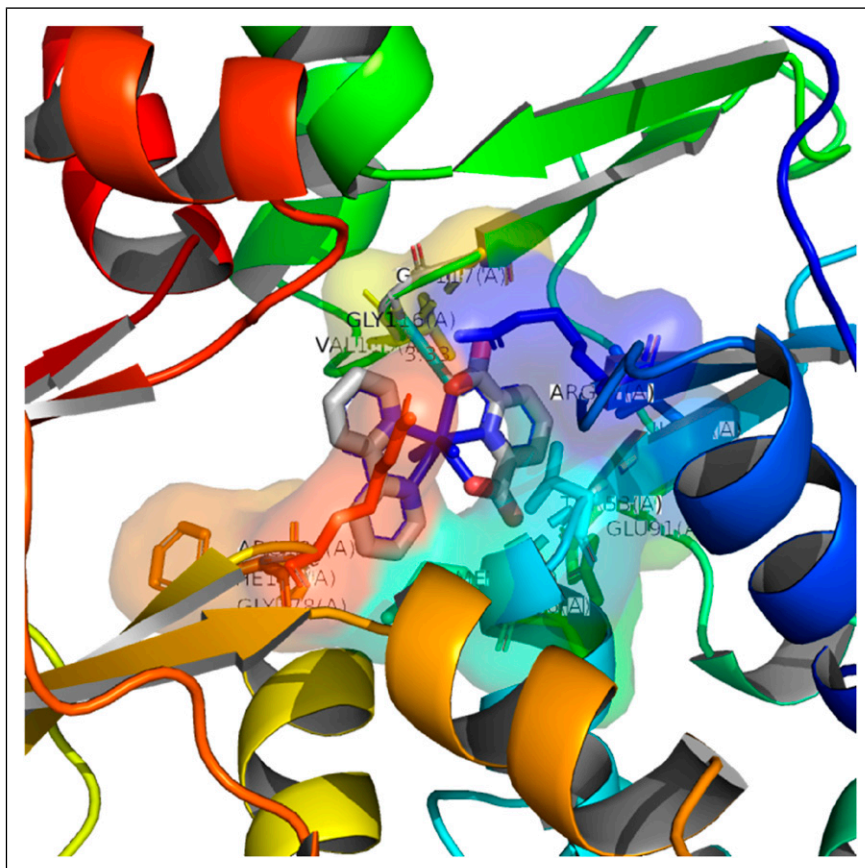
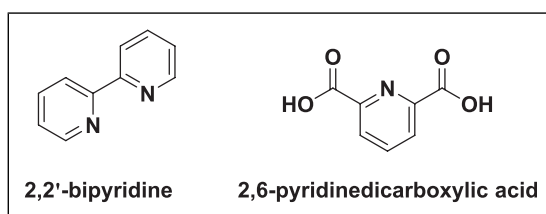


Figure 4. The local view of the environment of the captured binding conformation that exhibited the lowest affinity energy from 50 given binding poses. The interacting active residue and the potential active residues are listed explicitly.



Scheme 1 The chemical draws for the ligands used in this work.

groups have been observed to interact with the active residues and can be viewed as the origin of the biological capabilities.

Conclusion

Overall, we have produced $[\text{Bi}_4\text{Cl}_8(\text{PDC})_2(2,2'\text{-bpy})_4]\cdot 2\text{MeCN}$, the bismuth (III)-organic compound via using the solvothermal reactions between 2,2'-bipyridine; 2,6-pyridinedicarboxylic acid; and bismuth chloride. The **1**'s structure was investigated with the EA and the diffraction of single-crystal X-ray. The ELISA detection results reflected that our compound could obviously down-regulate the inflammatory cytokines released into the alveolar lavage fluid, dose-dependently. In addition to this, this compound also remarkably inhibited the AMPK signaling pathway activation in alveolar epithelial cells in a dose-dependent fashion. In the end, it can be found that our compound possesses outstanding application values on pediatric pneumonia by reducing the overactive inflammatory response. Although multiple pyridine rings are presented in the Bi complex, the simulation of molecular docking suggested that only the carboxyl groups have the capacity to interact with the active residues from the receptor protein.

Declaration of conflicting interests

The author(s) declared no potential conflicts of interest with respect to the research, authorship, and/or publication of this article.

Funding

The author(s) received no financial support for the research, authorship, and/or publication of this article.

Data Availability

The IR spectrum of complex **1** ([Supplementary Figure](#)), the information could be found in the supporting information file.

Supplemental Material

Supplemental material for this article is available online.

References

1. Lee H, Yun KW, Lee HJ, et al. Antimicrobial therapy of macrolide-resistant mycoplasma pneumoniae pneumonia in children. *Expert Rev Anti-infective Ther* 2018; 16: 23–34.
2. Kumar S. Mycoplasma pneumoniae: a significant but underrated pathogen in paediatric community-acquired lower respiratory tract infections. *Indian J Med Res* 2018; 147: 23–31.
3. Kumar S, Roy RD, Sethi G, et al. Mycoplasma pneumoniae infection and asthma in children. *Trop Doctor* 2019; 49: 117–119.
4. Patel AK, Jadeja RN, Roy H, et al. Pseudo-tetrahedral copper(II) complex derived from $\text{N}'\text{-}[(2\text{E},3\text{Z})\text{-}4\text{-hydroxy-4-phenylbut-3-en-2-ylidene}]\text{acetohydrazide}$: synthesis, molecular structure, quantum chemical investigations, antioxidant and antiproliferative properties. *J Mol Struct* 2019; 1185: 341–350.
5. Feng X, Li R, Wang L, et al. A series of homonuclear lanthanide coordination polymers based on a fluorescent conjugated ligand: syntheses, luminescence and sensor for pollutant chromate anion. *CrystEngComm* 2015; 17: 7878–7887.

6. Feng X, Feng Y, Guo N, et al. Series d-f heteronuclear metal-organic frameworks: color tunability and luminescent probe with switchable properties. *Inorg Chem* 2017; 56: 1713–1721.
7. Feng X, Feng Y-Q, Liu L, et al. A series of Zn-4f heterometallic coordination polymers and a zinc complex containing a flexible mixed donor dicarboxylate ligand. *Dalton Trans* 2013; 42: 7741–7754.
8. Hu ML, Abbasi-Azad M, Habibi B, et al. Electrochemical applications of ferrocene-based coordination polymers. *Chem Plus Chem* 2020; 85: 2397–2418.
9. Hu M-L, Razavi SAA, Piroozzadeh M, et al. Sensing organic analytes by metal-organic frameworks: a new way of considering the topic. *Inorg Chem Front* 2020; 7: 1598–1632.
10. Hu M-L, Safarifard V, Doustkhah E, et al. Taking organic reactions over metal-organic frameworks as heterogeneous catalysis. *Micropor Mesopor Mat* 2018; 256: 111–127.
11. Fan L, Zhao D, Li B, et al. An exceptionally stable luminescent cadmium(ii) metal-organic framework as a dual-functional chemosensor for detecting Cr(vi) anions and nitro-containing antibiotics in aqueous media. *Cryst Eng Comm* 2021; 23: 1218–1225.
12. Wang F, Tian F, Deng Y, et al. Cluster-Based multifunctional copper(II) organic framework as a photocatalyst in the degradation of organic dye and as an electrocatalyst for overall water splitting. *Cryst Growth Des* 2021; 21: 4242–4248.
13. Alvarez N, Mendes LFS, Kramer MG, et al. Development of copper(II)-diimine-iminodiacetate mixed ligand complexes as potential antitumor agents. *Inorg Chim Acta* 2018; 483: 61–70.
14. Vamsikrishna N, Daravath S, Ganji N, et al. Synthesis, structural characterization, DNA interaction, antibacterial and cytotoxicity studies of bivalent transition metal complexes of 6-aminobenzothiazole Schiff base. *Inorg Chem Commun* 2020; 113: 107767.
15. Che Z, Wang S, Liu S, et al. Facile green fabrication of nanostructure ZnO plates, bullets, flower, prismatic tip, closed pine cone: their antibacterial, antioxidant, photoluminescent and photocatalytic properties. *Spectrochim Acta A Mol Biomol Spectrosc* 2015; 135: 878–882.
16. Gomez GE, D'vries RF, Lionello DF, et al. Exploring physical and chemical properties in new multifunctional indium-, bismuth-, and zinc-based 1D and 2D coordination polymers. *Dalton Trans* 2018; 47: 1808–1818.
17. Yin G, Zeng Q, Zhao H, et al. Effect and mechanism of calpains on pediatric lobar pneumonia. *Bio-engineered* 2017; 8: 374–382.
18. Matthai J, Shanmugam N, Shanmugam N, et al. Coronavirus disease (COVID-19) and the gastrointestinal system in children. *Indian Pediatr* 2020; 57: 533–535.
19. Gomez-Garcia I, Oyenarte I and Martinez-Cruz LA. Structural and thermodynamic characterization of the TYK2 and JAK3 kinase domains in complex with CP-690550 and CMP-6. *J Mol Biol* 2010; 65: 813–817.